# Uplink Arraying Experiment with the Mars Global Surveyor Spacecraft

V. Vilnrotter,[1] D. Lee,[1] T. Cornish,[2] R. Mukai,[1] and L. Paal[2]

*For the first time ever, a pair of 34-m antennas was employed to simultaneously transmit and combine 7.15-GHz (X-band) carriers to a spacecraft in deep space, yielding up to four times greater signal power than either antenna separately. Antenna arrays have the potential to synthesize the equivalent of a very large antenna aperture in a robust and cost-effective manner, by appropriately combining the signals from a large number of smaller antennas. Prior to this experiment, only single 34-m or 70-m antennas had been used to uplink signals and commands to spacecraft. During this experiment, the Mars Global Surveyor spacecraft received the sum of the two carriers, measured the combined power level, and verified the predicted array gain resulting from the combining operation. Although great care had to be exercised to minimize differential Doppler between the two signals due to Earth rotation, it was demonstrated that the combined signal remained stable on timescales of 10 to 20 minutes, enabling the application of novel uplink array calibration algorithms, which may enable routine calibration of uplink arrays consisting of a large number of antennas in the future.*

## I. Introduction

Uplink arraying is a fundamentally new concept that promises to dramatically increase NASA's future deep-space communications capabilities. The requirements to command spacecraft after launch and during encounter, and to provide two-way communication and two-way ranging as well as in-flight reconfiguration to accommodate changes in mission objectives, are integral parts of every deep-space mission. The use of antenna arrays enables greater data rates, greater effective operating distance, and cost-effective scaling for more demanding future missions with a highly flexible design philosophy, via the inherently parallel architecture of antenna arrays.

The most advantageous uplink array configuration has not been determined at this time. Uplink arrays meeting the Deep Space Network's (DSN's) near-term requirements could be configured using only two or three 34-m antennas. Larger arrays of 10- to 12-m-diameter antennas also could be employed, and even larger arrays of still smaller antennas could be contemplated if compelling enough reasons were found. When this 34-m uplink array prototype demonstration effort is completed, the DSN will essentially have a three-element uplink array, each with its own operational 20-kW transmitters, transmitting at the exact

[1] Communications Architectures and Research Section.

[2] Communications Ground Systems Section.

The research described in this publication was carried out by the Jet Propulsion Laboratory, California Institute of Technology, under a contract with the National Aeronautics and Space Administration.

frequency band currently employed by the DSN. The calibration techniques developed with this 34-m demonstration array can be applied to arrays of smaller antennas and may employ near-Earth space assets (such as a dedicated uplink array calibration module on a future geostationary satellite or even on the surface of the Moon). All necessary functional components of an operational uplink array can be explored with the proposed 34-m array prototype, including signal distribution over realistic distances, dynamic tracking of far-field sources close to the ecliptic (where most NASA spacecraft orbit), and taking into account the effects of time-varying geometry affecting differential Doppler and modulation delay. These dynamic components pose some of the greatest challenges to uplink arraying; hence, they must be addressed in an environment as close to actual operational conditions as possible for the uplink array demonstration.

Although 7.15-GHz (X-band) uplink is performed routinely using operational 34- and 70-m antennas, fundamental limitations in practically attainable antenna aperture and safety-constrained transmitter power relegate the single-antenna uplink approach to modest distances and command rates. This has implications not only for the operational range of single-aperture uplink antennas, but also for the time it takes to regain communications with spacecraft in case of emergency. The higher power density provided by the uplink array in the vicinity of the spacecraft requires shorter dwell times, hence faster scanning of the uncertainty cell, enabling faster recovery of communications with the spacecraft. However, since uplink arraying has never been demonstrated before at interplanetary distances, it is essential to develop and successfully demonstrate the key technologies before committing to any particular uplink array design.

Following current DSN practices, it is assumed that an operational uplink array calibration will take place before each track, and that the array will be required to maintain calibration throughout the track. After uplink array calibration is achieved, local measurements of antenna phase will be employed to minimize instrumental and fiber-optic phase drift. The calibrated phase vector will be recomputed for the spacecraft look direction, or line of sight (LOS), using ephemerides and knowledge of the antenna phase centers. Note that the availability of a downlink signal suitable for array calibration cannot be assumed in general.

Arraying of receiving antennas for downlink reception is the subject of several ongoing efforts, and 34-m antennas have already been arrayed previously to enhance reception performance of Galileo downlink signals. The objectives of the current Mars Global Surveyor (MGS) Uplink Arraying Experiment were as follows:

(1) Demonstrate far-field maximization of uplink array signal power at the spacecraft

(2) Show that uplink power at the spacecraft increases by 6 dB when equal powers are transmitted

(3) Demonstrate differential phase-ramp optimization algorithms designed to estimate the required phase offsets based on spacecraft automatic gain control (AGC) measurements

(4) Determine the degradation in received power due to uncompensated phase drift

(5) Attempt to maintain phase alignment of the two uplink signals using active phase control on the ground

The uplink arraying functions demonstrated and evaluated during this experiment include (1) removal of differential Doppler from the transmitted X-band uplink carriers; (2) differential phase ramping of transmitted X-band carriers; (3) spacecraft configuration to deliver AGC readings as part of engineering data; (4) AGC readings obtained in real time from downlink telemetry and processing of engineering data to extract the sequence of AGC readings; (5) real-time analysis of spacecraft data to estimate the optimum uplink array differential phase; (6) application of optimum differential phase to the uplink signals; and

(7) real-time monitoring of phase drifts in the ground equipment. Alternate approaches to uplink array calibration, including Doppler-delay processing of reflected signals from the Moon, have been reported previously in [1,2].

## II. MGS Uplink Array Experiment Description

The goal of this experiment was to illuminate the MGS spacecraft simultaneously with two unmodulated X-band carriers, from two 34-m beam-waveguide (BWG) antennas at Goldstone, Deep Space Stations 24 and 25 (DSS 24 and DSS 25), and to determine the stability of the arrayed carrier power at the spacecraft. A conceptual block diagram of the experiment setup is shown in Fig. 1, utilizing three distinct antennas for clarity. In the actual experiments, one of the transmit antennas (DSS 25) was configured to transmit X-band uplink as well as receive MGS downlink telemetry.

The profile of the differential Doppler caused by Earth rotation for the two antennas employed in these experiments is shown in Fig. 2. The differential Doppler was removed by the use of accurate frequency predicts applied to the exciters at Signal Processing Center 10 (SPC 10) prior to transmission in order to generate a stable far-field signal. With two antennas, the arrayed power distribution in the far field is the product of the primary antenna pattern and the interference pattern generated by two point sources located at the antenna phase centers, an example of which is shown in Fig. 3. In addition to differential Doppler compensation, time-varying frequency due to the orbital trajectory of MGS around Mars also was removed using frequency predicts, in order to minimize stress on the transponder's phase-locked loop.

Pointing of the two antennas toward the spacecraft to a small fraction of the primary beamwidth is routinely achieved with the operational antennas at the Apollo complex. However, this does not guarantee that the peak of the interference pattern generated by the two-antenna array is actually illuminating the spacecraft; the transmitted phases must be aligned at the spacecraft in order to achieve combined power maximization. Initially, the spacecraft may be located near a peak or a null of the two-antenna interference pattern, but most likely at some intermediate point on the array gain profile. An example of the far-field power distribution generated by a two-antenna array, perpendicular to the baseline, is shown in Fig. 3.

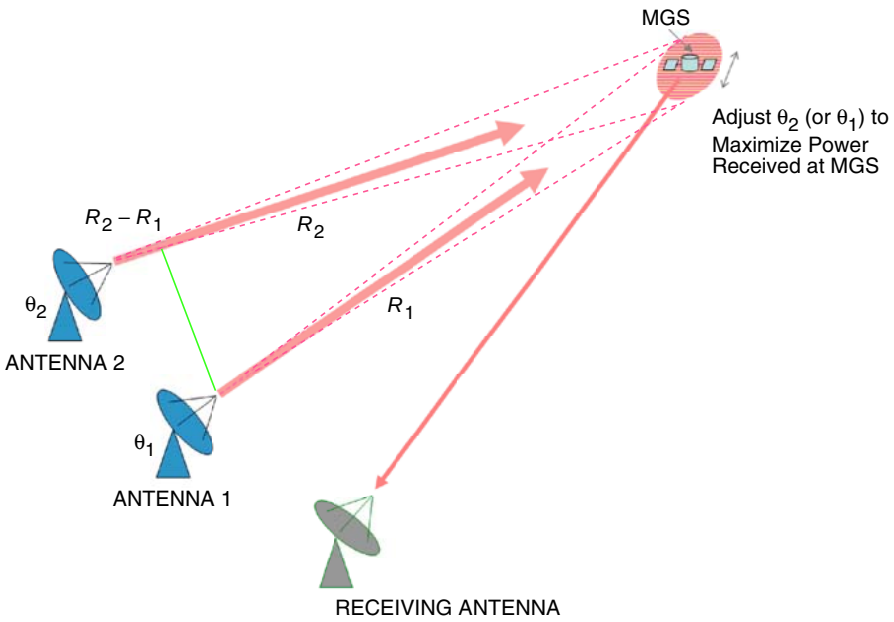


**Fig. 1. MGS uplink array experiment conceptual block diagram.**

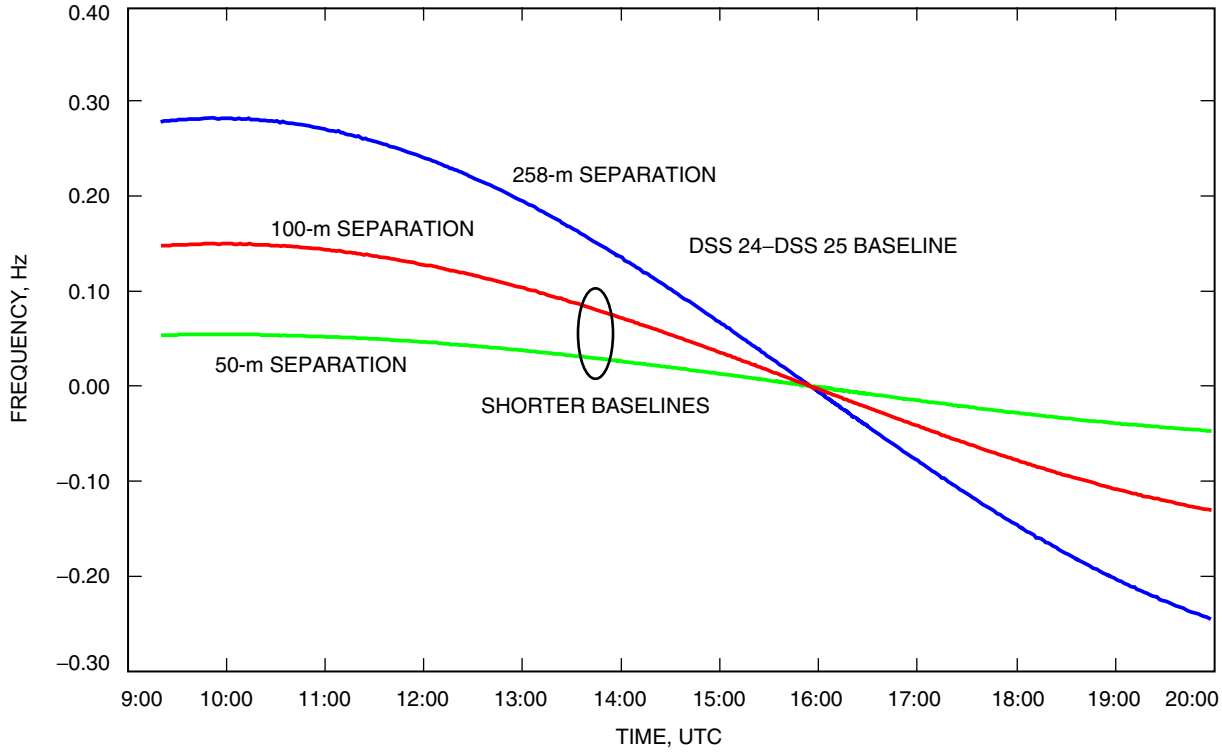


**Fig. 2. Examples of DSS-24/DSS-25 differential Doppler to MGS versus antenna separation.**

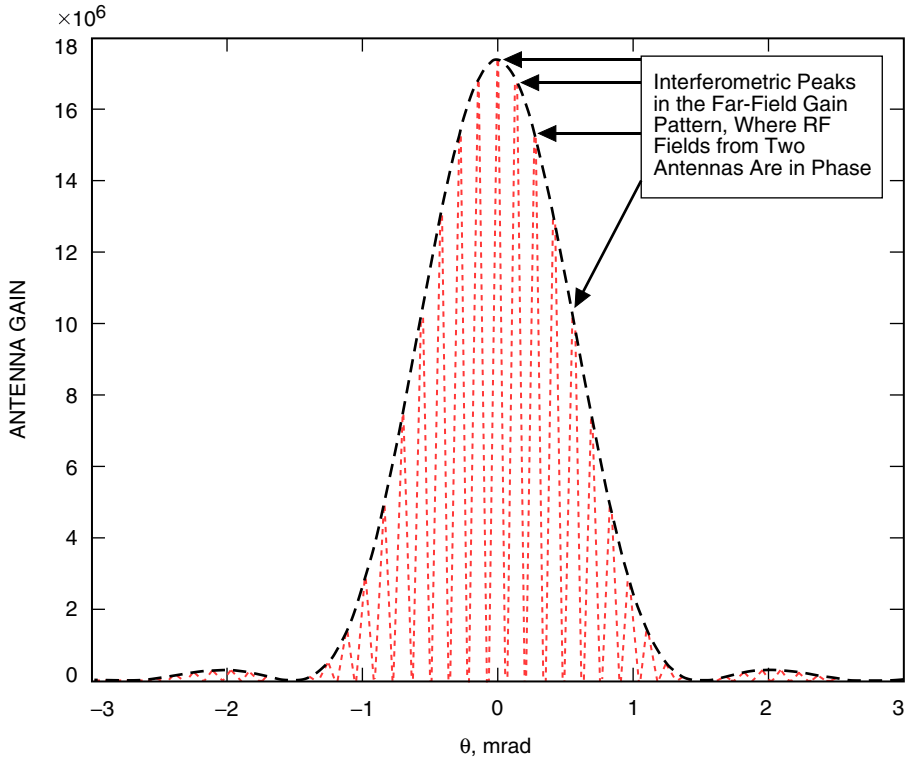


**Fig. 3. Far-field pattern of two-element array (34-m diameter, separated by 300 m).**

Note that peaks and nulls occur closely spaced in the interference pattern, requiring precise electronic beam steering to illuminate MGS with the peak of the array pattern.

Two 34-m BWG antennas at Goldstone were scheduled to track MGS using frequency predicts generated by mission operations. The DSS-25 transmitter was commanded to radiate a 10-kW X-band carrier, and the uplink frequency was swept to ensure that the spacecraft transponder acquired the signal. After the MGS transponder locked up, the DSS-25 ground station receiver also acquired and locked onto the downlink carrier and began recording engineering telemetry from the spacecraft. The engineering telemetry contained readouts from the AGC, which provided near-real-time measurement of the received uplink carrier power.

The DSS-24 transmitter was configured to transmit a 3-kW carrier. However, it was found that the phase modulator in the DSS-24 signal path introduced changes in the actual output power, which varied by ±200 W around a mean value of 3.3 kW during the experiment. This antenna was initially configured for a lower uplink power so that the spacecraft transponder could stay locked to the uplink carrier even if the carrier phases happened to arrive 180 deg out of phase. When properly phased up at the spacecraft, arraying of 10-kW and 3.3-kW transmitters yields an equivalent power of approximately 25 kW at the spacecraft, yielding a gain of 4 dB over the 10-kW antenna. This theoretical gain is somewhat surprising at first, but we need to recall that it is the amplitudes, not the powers, that are added with coherent combining. Therefore, in the far field the transmitted power levels are proportional to the square of the sum of the amplitudes: $P_t \propto \left(\sqrt{3,300} + \sqrt{10,000}\right)^2 = (57.45{+}100)^2 = 24,790$ watts when the transmitted fields are added in phase at the spacecraft. When both antennas transmit equal-power, phase-aligned carriers, the received power is theoretically 6-dB greater than would be received from either antenna separately. The variation of the combined power with differential phase, for different power levels, is shown in Fig. 4, where $\Delta P = P_{\min}/P_{\max}$ is the ratio of the smaller transmitted power to the larger, in decibels. Figure 5 shows the calibration curve for the 8-bit receiver AGC; note that the calibration curve is reasonably linear in the region of interest, nominally −110 dBm to −135 dBm, implying that we can expect accurate power readings in this region during the experiment.

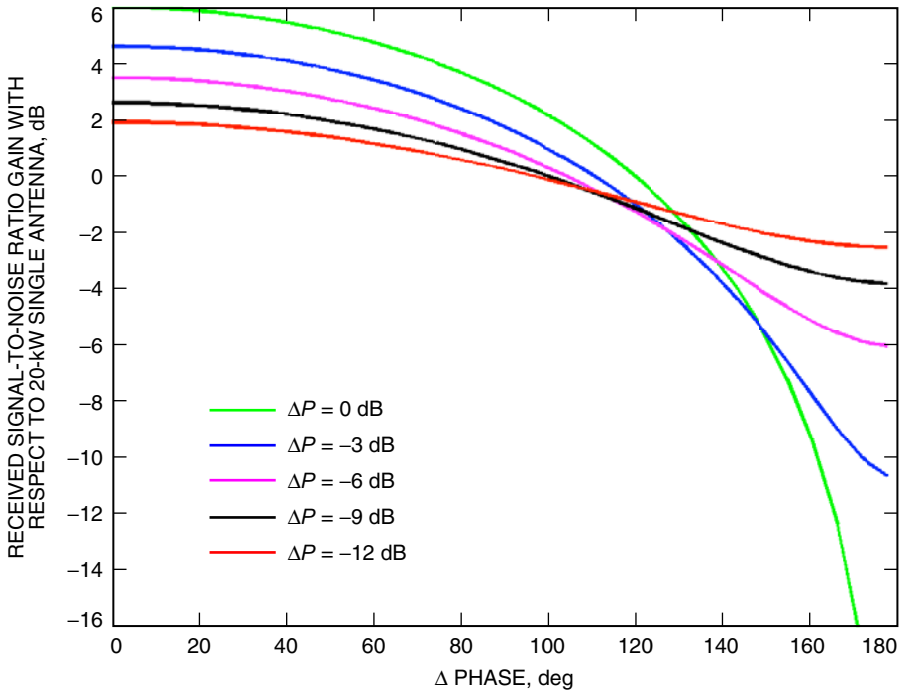


**Fig. 4. Uplink array gain for various power ratios, $\Delta P$, as a function of carrier phase difference.**

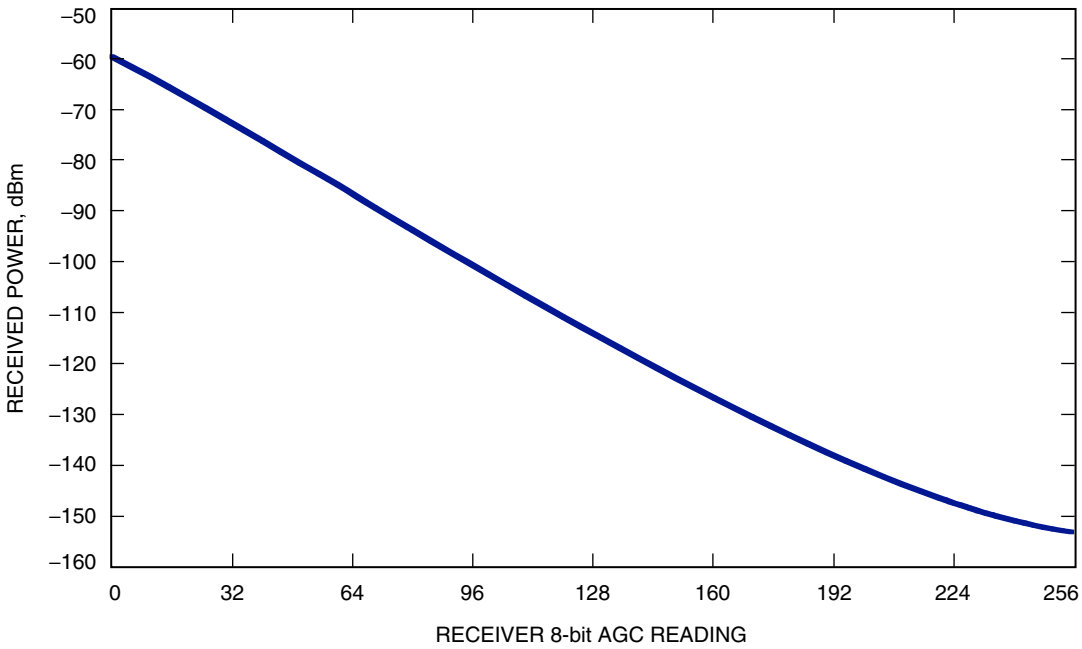


**Fig. 5. Mars Observer transponder 2 (MOT2) receive AGC calibration curve.**

Figure 6 shows the MGS–Earth range (dark blue) and round-trip light time (RTLT, pink) from December 28, 2005, to July 26, 2006. When the experiment took place on February 25, 2006, the range was approximately 200 million kilometers, which corresponds to an RTLT of 22 minutes. Figure 7 shows anticipated combined power levels received at MGS for different uplink array configurations during the same time interval. With DSS 25 configured for 10-kW uplink (dark blue), the received power at the spacecraft is expected to be approximately −127 dBm. When the 3.3-kW transmitted field from DSS 24 reaches MGS, the maximum combined power should increase by 4 dB; hence, the phased-up received power is expected to be −123 dBm. For spacecraft safety reasons, the full 20-kW powers of the two antennas were not used in this experiment, even though the maximum resulting power would not exceed −118 dBm, which is much less than the maximum permitted power level at the spacecraft.

Figure 8 shows the expected downlink $P_t/N_0$ for a 2000 bits per second (bps) downlink from MGS during the same time interval. The Block V receiver threshold is 36 dB-Hz, which is more than sufficient for error-free detection of the downlink telemetry in this experiment. The far-field intensity produced by the two-antenna uplink array can be steered over the spacecraft electronically from the ground by varying one of the transmitter phases. When the differential phase is varied over the entire range of $(0, 2\pi)$ radians, it is guaranteed that the peak of the intensity pattern illuminates the spacecraft, provided the phases are stable over the duration of the sweep. This power variation can be measured by the AGC to monitor the instantaneous carrier power at the spacecraft. The results of these measurements then are relayed to the ground as engineering data and evaluated to determine the optimal phase adjustment required to phase up the signals at the spacecraft. Note that downlink reception during this experiment was not carried out by a separate antenna, as indicated in the concept diagram of Fig. 1. Instead, the X-band receiver of the DSS-25 antenna was tuned to the downlink frequency and used to monitor the MGS telemetry.

The two 34-m BWG antennas assigned to transmit to MGS used Network Support Subsystem (NSS) predicts generated by mission operations. The DSS-25 transmitter was commanded to radiate a 10-kW

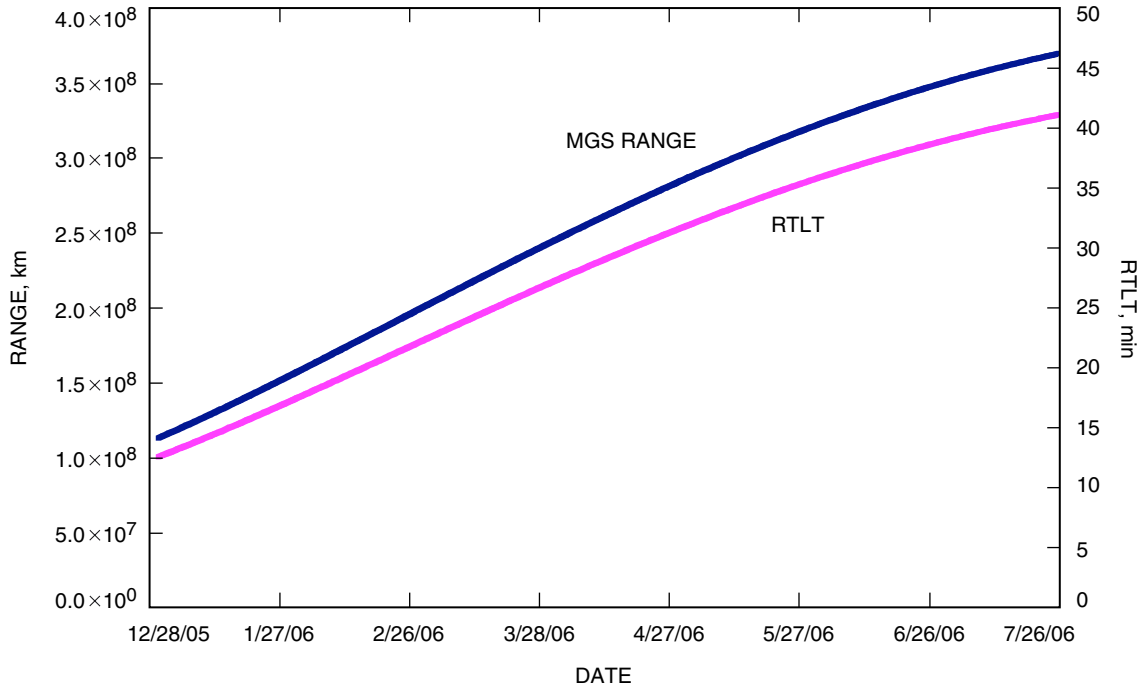


**Fig. 6. MGS range and RTLT.**

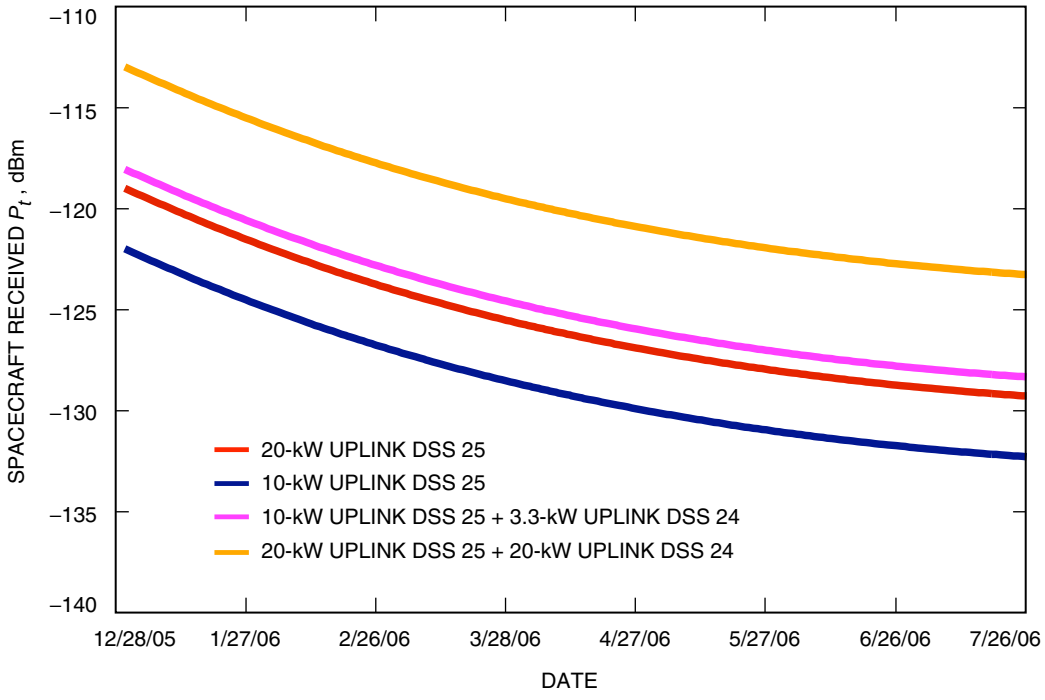


**Fig. 7. MGS spacecraft received power.**

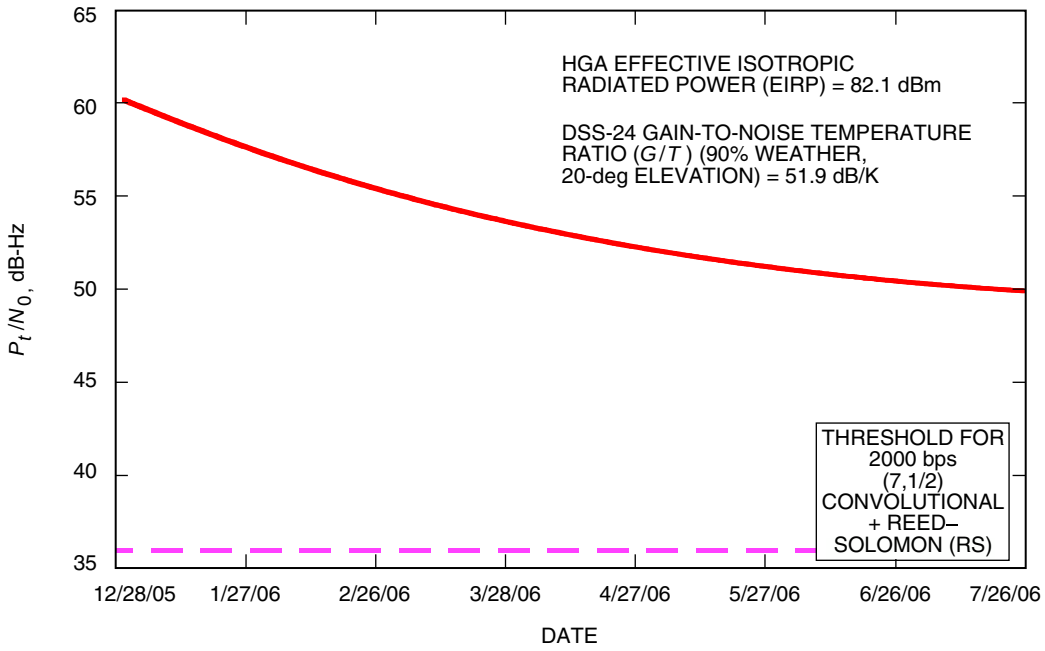


**Fig. 8. MGS downlink $P_t/N_0$.**

X-band carrier of nominally 7.15 GHz plus Doppler compensation, whereas the DSS-24 carrier power was 3.3 kW to ensure that sufficient power would reach the spacecraft, regardless of the initial phase between the two signals. The DSS-25 ground station receiver acquired and locked to the MGS downlink carrier, which was configured for one-way operation, and began recording engineering telemetry from the spacecraft. After confirmation that the spacecraft was locked to the uplink carrier, the DSS-24 transmitter started transmitting 3.3 kW of X-band carrier at the same nominal frequency, but differing somewhat due to differential Doppler. It was anticipated that the second antenna initially would be out of phase with the 10-kW DSS-25 carrier; however, due to the unequal transmitted powers, the spacecraft transponder would be able to stay in lock even if the uplink carriers were 180 deg out of phase. The worst-case power level seen by the spacecraft can be computed as $P_t = \left(\sqrt{10,000} - \sqrt{3,300}\right)^2 = (100 - 57.45)^2 = 1811$ watts, which is sufficient to maintain lock. Note that the out-of-phase power is a factor of 5.5, or 7.4 dB, less than the 10 kW power of the DSS-25 transmitter alone. In an operational setting, the intent with a two-antenna array is to generate 6-dB greater power at the spacecraft than with a single antenna. This 6-dB array gain was also demonstrated towards the end of the experiment by increasing the power of the DSS-24 transmitter to equal that of the DSS-25 transmitter.

The engineering telemetry contains readouts from the spacecraft receiver AGC, providing a measurement of the received uplink signal power. Since the phases of the DSS-24 and DSS-25 exciters are unknown a priori, an X-band phase modulator at SPC 10 was used to slowly ramp the DSS-24 uplink phase. Figure 9 is a block diagram of the phase modulator setup, providing differential Doppler compensation through the use of separate exciters at SPC 10, one for each transmitting antenna.

Because the transmitter phases at DSS 24 and DSS 25 were expected to vary slowly due to temperature variations and equipment drift, phase measurements were taken at the maxima and minima of the frequency trajectories, dominated by MGS orbital dynamics with a period of approximately 2 hours. The round-trip phase comparator assembly compared the phase of the X-band carrier at the exciter output with a sample of the carrier at the output coupler of the power amplifier at each antenna. This yields a stable measurement of the round-trip phase when the frequencies are not changing; however, the frequency did change between trajectory peaks, requiring compensation for the different number of

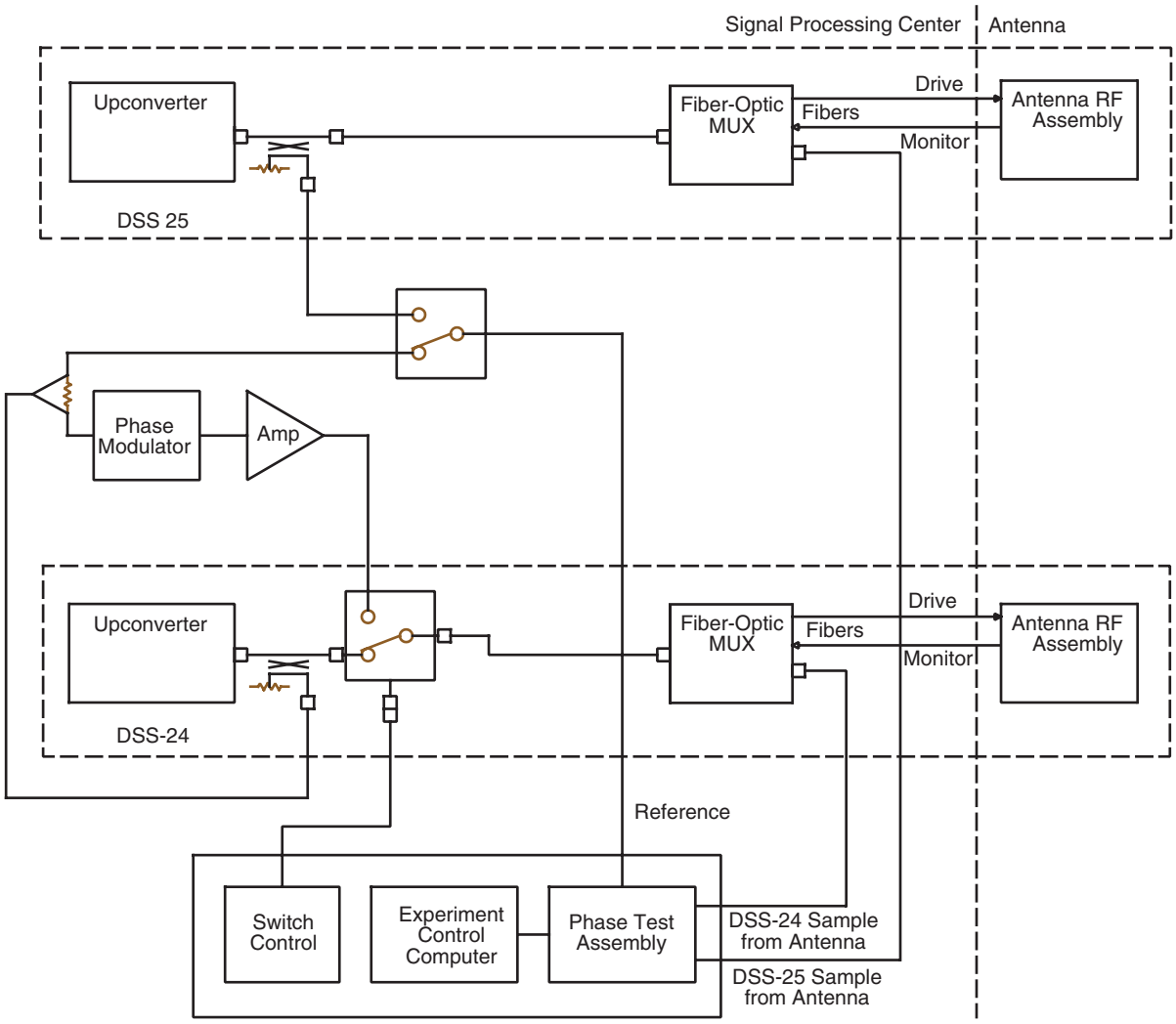


**Fig. 9. DSS-24 phase modulator configuration at SPC 10.**

carrier wavelengths supported by the electrical pathlength. Although an attempt was made to take this effect into account, the accuracy of the phase estimate was dominated by the uncertainty in the electrical pathlength; hence, it was decided not to compensate for local phase variations during this experiment.

## III. MGS Uplink Array Experiment Results

The uplink carrier phase at DSS 24 was ramped from 0 to $2\pi$ rad using the phase modulator, and the spacecraft AGC readings were monitored at SPC 10. On the MGS spacecraft, an AGC reading was taken every 16 seconds, with a resolution of 0.3 to 0.4 dB, which was deemed adequate for this experiment. The AGC samples were continuously transmitted to DSS 25 when the spacecraft was visible, and they were observed one light time later at SPC 10 on a workstation monitor. The first AGC readings arrived on schedule, indicating received powers of approximately $-126$ dBm from DSS 25, as predicted. Soon thereafter the power reading was seen to increase as the second signal transmitted from DSS 24 reached MGS. Because the station configuration was not fully optimized to support uplink arraying, the frequency predicts used during this experiment contained some periods of large phase shift (estimated to be as large as $\pm 65$ deg) but also contained phase-stable regions. These differential phase errors, resulting

from frequency errors in the predicts, are believed to be a significant contribution to the total phase error between the two X-band carriers. A comparison of the phase drift due to frequency predict errors and the actual phase difference estimated from the AGC data during part of the second orbit is shown in Fig. 10, indicating good correlation between the smooth phase predicts and the noisier phase estimates obtained from the AGC readings.

Phase ramping was performed to determine the optimum phase, resulting in an increase in measured array power from approximately −126 dBm to −122 dBm, confirming the 4-dB predicted gain. Examples of the preamble (phase jumps of 90 and 270 degrees every 40 seconds), fast phase ramp (0 to 360 degrees in 4 minutes), and slow phase ramp sequences (0 to 360 degrees in 11 minutes) performed during the first orbit are shown in Fig. 11. The fast ramp yielded a rough measurement of 60 degrees for the optimum phase, while the finer slow ramp yielded 64 degrees, in good agreement. Note that the peaks of the ramps range from −122 dBm to −123 dBm in Fig. 11, in agreement with predictions and also consistent with the 0.3- to 0.4-dB measurement accuracy of the AGC, due primarily to quantization.

The entire second orbit was devoted to passive measurement of signal power and phase difference at the spacecraft, in order to characterize phase fluctuations due to predict errors, thermal effects, and equipment drift on the ground. A fast ramp was performed at the beginning, at the middle, and near the end of the second orbit. The middle measurement occurred during a period of near-perfect phase alignment and relatively stable phase, as can be seen in Fig. 12; the maximum combined power observed during this phase ramp was −123 dBm, close to the theoretical maximum, and indeed the phase ramp yielded an optimum phase measurement of approximately 0 degrees, as required for maximum combined power. Following the phase ramp, the combined power remained close to its maximum value, −122 dBm to −123 dBm, for more than 10 minutes. This level of differential phase stability from NSS frequency predicts designed only for single-antenna uplink transmissions was somewhat surprising, and attests to the accuracy of the NSS frequency predicts. Future experiments will employ even better Service Preparation Subsystem (SPS) predicts, which should remain stable over the entire track.

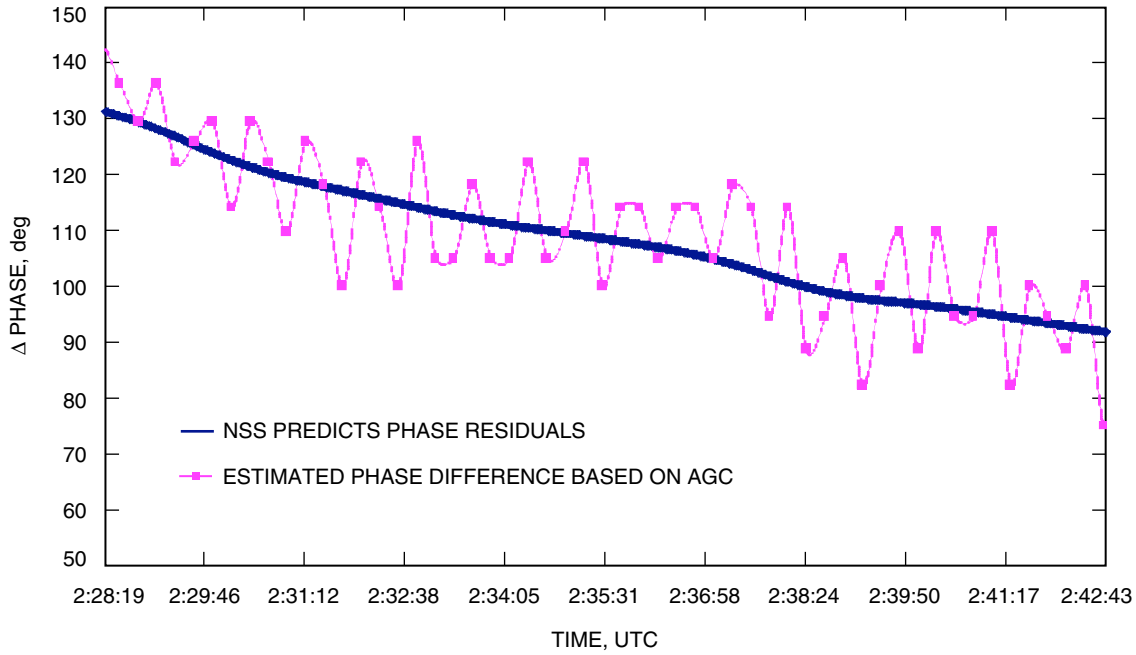


**Fig. 10. Comparison of predicted and measured phase difference at MGS.**

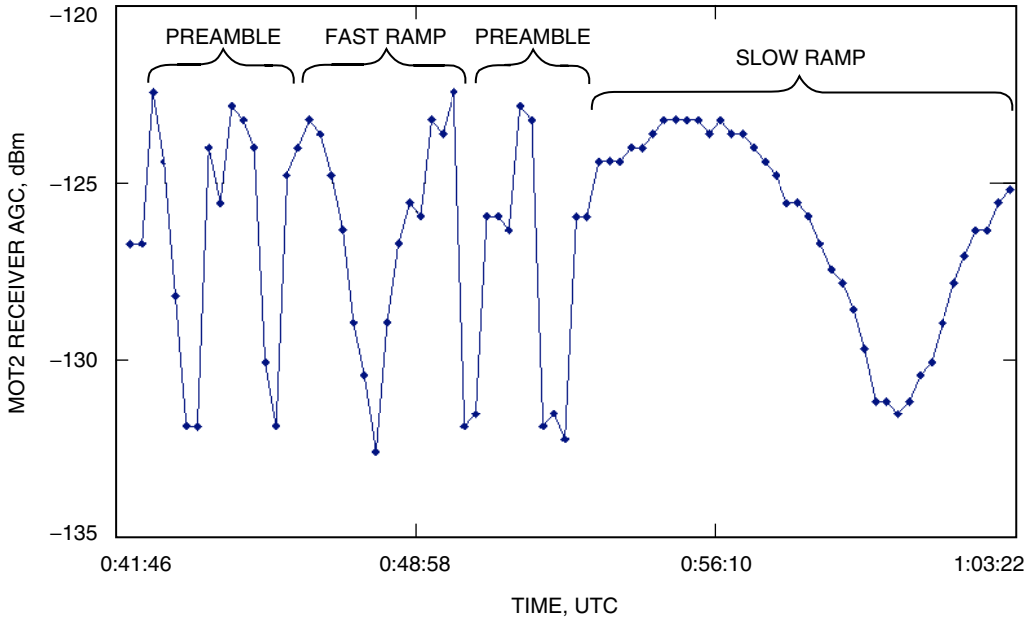


**Fig. 11. Examples of fast and slow phase-ramp sequences for estimating optimum phase.**

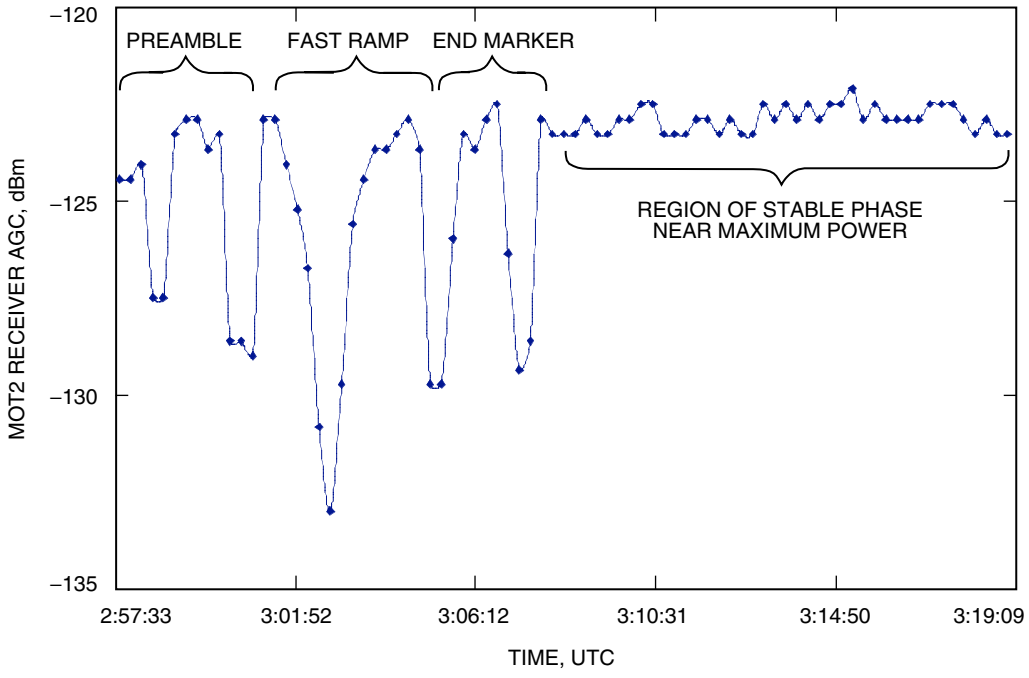


**Fig. 12. Examples of fast-ramp and stable differential phase near maximum power.**

An interesting test during the third orbit was the application of a 180-deg phase shift after power was maximized to verify the expected 11.4-dB drop in combined power; this power drop can be seen clearly in Fig. 13. Finally, during the fourth orbit, the DSS-24 transmit power was increased slowly from 3.3 kW to 10 kW, resulting in a further 2-dB power gain at the spacecraft. This is shown in Fig. 14, where the maximum combined power reached around 7:14:53 UTC is indeed close to the predicted maximum of −120 dBm. The slow increase in received power during the first half of Fig. 14 was due to phase ramping as the transmitter power was increased to 10 kW at DSS 24.

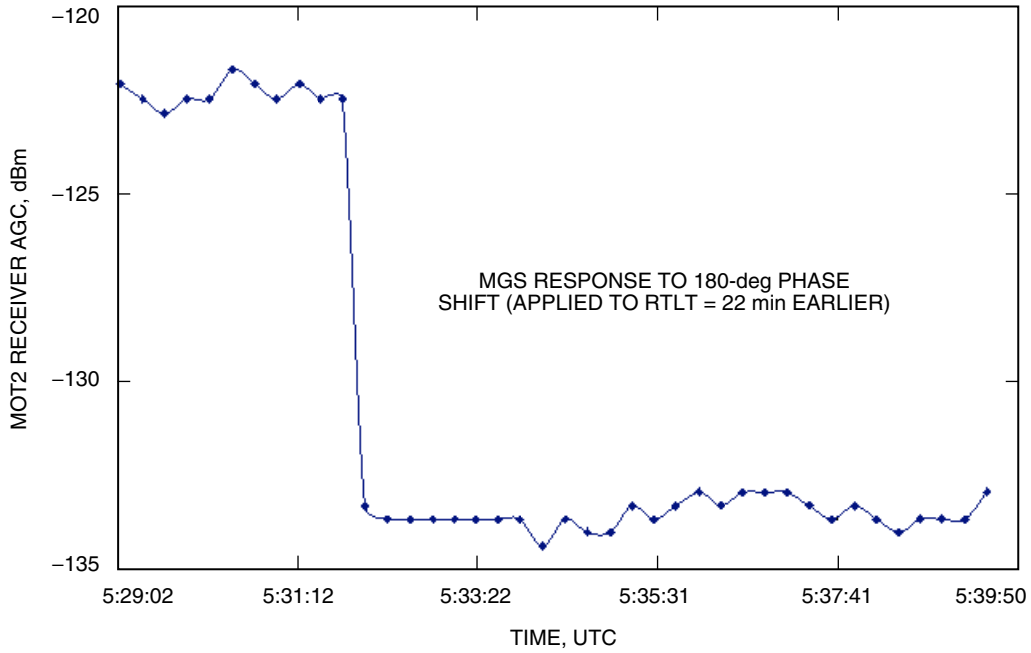


**Fig. 13. Demonstration of constructive and destructive interference with 3 and 10 kW.**

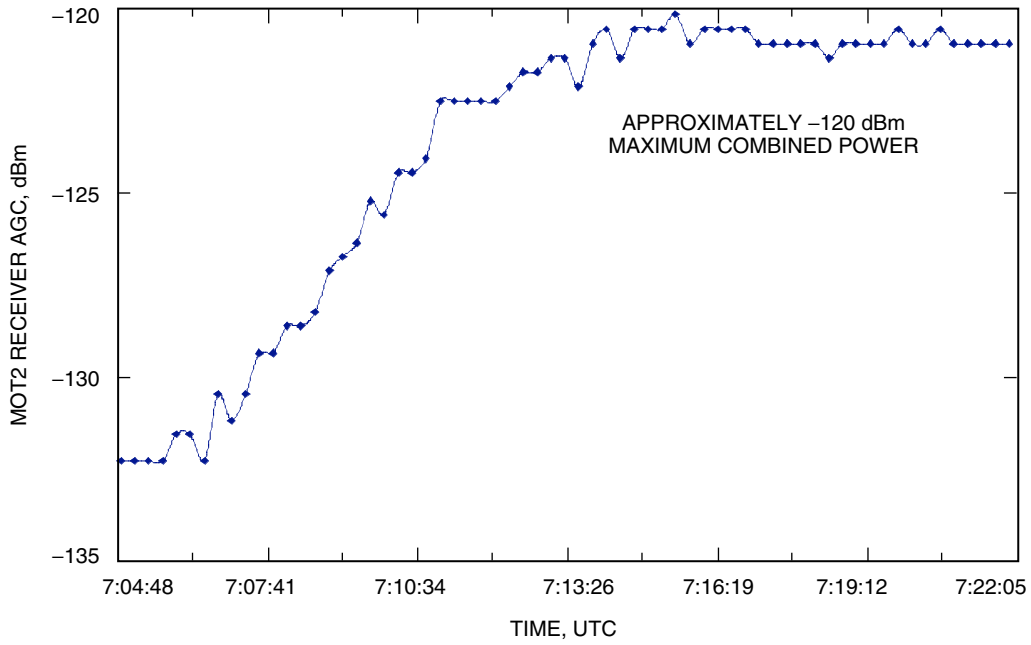


**Fig. 14. Demonstrating maximum combined power of −120 dBm.**

The recorded AGC readings were post-processed to illustrate what readings would have been obtained if unwanted phase drifts during the experiment were greatly reduced, either through better predicts or through more accurate local phase control. After the optimum phase of 60 deg was determined from a slow ramp applied during the first orbit, a 60-deg phase offset was applied to the DSS-24 carrier using the phase modulator assembly illustrated in Fig. 9. After 22 minutes of RTLT, the response of the AGC power reading was observed to drop to −132 dBm instead of increasing to its maximum value of −122 dBm, as it should have in the absence of phase drift after the phase measurement and during the one-way light time. A plot of the recorded data is shown in Fig. 15 as the dashed gray line labeled "Unprocessed AGC Readings." However, after post-processing the data to remove a linear phase drift component estimated directly from the AGC readings, the solid pink line in Fig. 15 shows that in the absence of phase drift the application of 60 deg of phase to the DSS-24 signal indeed would have maximized the received power at the spacecraft, resulting in a combined power of approximately −122.5 dBm of received power. It is expected that this will be demonstrated during future experiments, which will employ improved SPS frequency predicts, as well as real-time monitoring of local phase.

## IV. Conclusions and Future Research

The first-ever demonstration of carrier arraying of two X-band signals at interplanetary distances has been demonstrated in a two-antenna arraying experiment with the MGS spacecraft, on February 25, 2006. The experiment was carried out under realistic operational conditions at the Goldstone Deep Space Communications Complex, using the 34-m BWG antennas located at DSS 24 and DSS 25 in the Apollo complex. Doppler-compensated X-band carriers were transmitted to the MGS spacecraft in orbit around Mars, and the concept of phase optimization to maximize received power was demonstrated through the use of a novel phase-ramp algorithm. Power maximization was achieved temporarily during each phase ramp, validating the predicted array gain, and data were collected to characterize the residual phase-drift components. It was observed that despite severe diurnal and Mars-orbital dynamics, differential phase remained stable on time scales of 10 to 20 minutes, indicating that further improvements in frequency

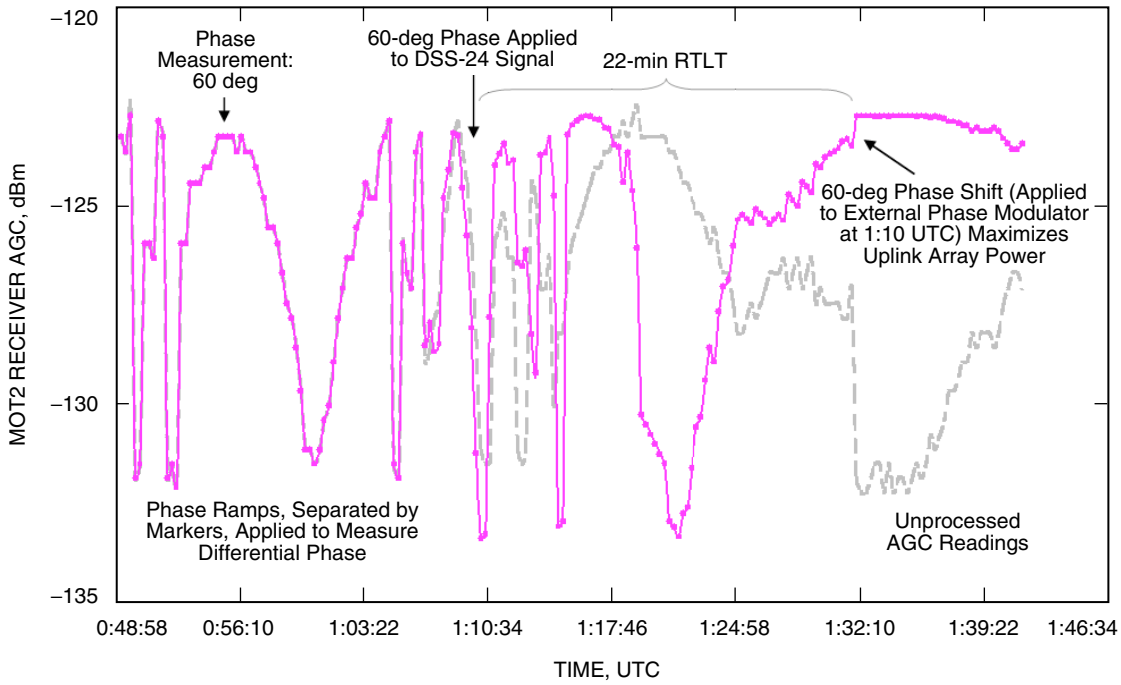


**Fig. 15. Post-processed AGC readings compensated for phase drift.**

predicts and local phase-measurement techniques should result in stable operation over a time scale of hours. Follow-on experiments are planned in the future to refine these techniques. The focus of the follow-on experiments will be to extend these preliminary results by demonstrating stable maximized power at the spacecraft for an entire orbit or more.

## Acknowledgment

The authors would like to thank Faramaz Davarian for numerous helpful suggestions during the course of this experiment and for helping to coordinate the experiment with MGS Mission Operations.

## References

[1] V. Vilnrotter, R. Mukai, and D. Lee, "Uplink Array Calibration via Far-Field Power Maximization," *The Interplanetary Network Progress Report*, vol. 42-164, Jet Propulsion Laboratory, Pasadena, California, pp. 1–16, February 15, 2006. http://ipnpr.jpl.nasa.gov/progress_report/42-164/164D.pdf

[2] F. Davarian and V. Vilnrotter, "Uplink Antenna Arraying for the Interplanetary Network," *Proceedings of the 24th AIAA International Communications Satellite Systems Conference (ICSSC)*, San Diego, California, June 10, 2006.